Induced magnetic field computations using a boundary integral formulation

S. Balac[(1)] and G. Caloz[(2)]

[(1)] Département de Mathématiques, Université de Bretagne Occidentale,
29285 Brest, France (Stephane.Balac@univ-brest.fr)

[(2)] Institut de Recherche Mathématiques de Rennes, Université de Rennes 1,
35042 Rennes, France (Gabriel.Caloz@univ-rennes1.fr)

Abstract

A method to compute the magnetic field induced by a metallic body embedded in a uniform external field is presented. It is based on boundary integral representation formulae for the magnetic induction $\overrightarrow{B}$. A computational procedure is proposed which consists in using analytic expressions to compute the integral over the flat panels of the boundary and a piecewise quadratic interpolation of the surface for the curved panels. Superconvergence occurs in the latter case. The method supplies both high accuracy and low computation time, requirements that are not fulfilled when using standard numerical methods.

1 Introduction

Our goal is to develop a method to compute the magnetic field induced by a metallic body either paramagnetic or diamagnetic embedded in a uniform external magnetic field. We encounter such problems in Magnetic Resonance Imaging (MRI) where the metallic body is a medical implanted device (orthopedic device, dental implant, ...) and the external magnetic field is one of the fields used to produce the image. In a MRI experiment, the metallic body produces an induced magnetic field that perturbs the magnetic field, resulting in a distortion of the image. Such distortions (called artifacts) may render the clinical diagnosis impossible. Numerical simulations appear to be a valuable tool to study and prevent MRI artifacts. In fact in the whole numerical simulation process, magnetic field computations are linked with image reconstruction algorithms; that is why we need to provide a high accuracy and low computation time method to compute the induced magnetic field.

So we have developed an efficient method taking advantage of the fact the metallic body is a paramagnetic material, so that an integral representation formula can be used for the induction. The computation of the magnetic field is then reduced to the evaluation of an integral over the body boundary. One major advantage of this approach is the fact the integral can be evaluated exactly for the flat boundary parts leading to accurate and fast computed results. For the curved parts of the boundary, the integral is evaluated numerically. First we approximate the boundary by a piecewise quadratic interpolation of a curvilinear triangulation of the surface. Then we use a quadrature rule over each quadratic interpolated triangle.

Our paper is organized as follows. In Section 2 we present the notations and the magnetostatic problem under consideration, while in Section 3 we present our approximation method. Section 4 is devoted to a careful error analysis. In particular we prove that the order of convergence is h^4 which is higher than what would be expected based on the underlying interpolation theory, namely h^3. This superconvergence result is due to cancellation of terms in the development of the error for pairs of symmetric triangles. A similar phenomenon was already observed by D. Chien and K. Atkinson, see [3] and [7], with a piecewise polynomial collocation method for integral equation on a surface in $\mathbb{R}^3$. Finally in Section 5 we present numerical results to illustrate the method.

2 The magnetostatic problem

Let us briefly describe the magnetostatic problem under consideration. Ω is an open bounded domain in $\mathbb{R}^3$, whose boundary is denoted by Σ. The metallic body Ω is embedded in a constant magnetic field $\overrightarrow{B_0}$. Let $\overrightarrow{B}$ be the magnetic flux density and $\overrightarrow{H}$ be the magnetic field intensity. The basic equations of magnetostatics are

$$\left\{ \begin{array}{rcl} \operatorname{div} \overrightarrow{B} & = & 0 \text{ in } \mathbb{R}^3, \\ \operatorname{rot} \overrightarrow{H} & = & 0 \text{ in } \mathbb{R}^3. \end{array} \right. \tag{1}$$

At a distance far from Ω the magnetic field tends to become homogeneous; we have

$$\lim_{|x|\to\infty} \overrightarrow{B}(x) = \overrightarrow{B_0}. \tag{2}$$

In the exterior region $\Omega' = \mathbb{R}^3 \setminus \overline{\Omega}$, $\overrightarrow{H}$ and $\overrightarrow{B}$ are related through the relation

$$\overrightarrow{H} = \frac{1}{\mu_0} \overrightarrow{B}, \tag{3}$$

where μ_0 is the magnetic permeability of vacuum, while in Ω they are connected to the magnetization $\overrightarrow{M}$ by the relation

$$\overrightarrow{H} = \frac{1}{\mu_0} \overrightarrow{B} - \overrightarrow{M}. \tag{4}$$

For the magnetic flux induction $\overrightarrow{B'} = \overrightarrow{B} - \overrightarrow{B_0}$ the problem reads: find $\overrightarrow{B'} \in L^2(\mathbb{R}^3)^3$ such that

$$\left\{ \begin{array}{rcl} \operatorname{div} \overrightarrow{B'} & = & 0 \text{ in } \mathbb{R}^3, \\ \operatorname{rot} \overrightarrow{B'} & = & 0 \text{ in } \Omega \text{ and } \Omega', \\ [\overrightarrow{B'} \wedge \overrightarrow{n}] & = & \mu_0 (\overrightarrow{M} \wedge \overrightarrow{n}) \text{ at the interface } \Sigma, \end{array} \right. \tag{5}$$

where $\overrightarrow{n}$ is the unit outward normal to Σ and $[\cdot]$ denotes the jump across the boundary Σ. To deal with a well posed problem we still need to add some relation between the magnetization $\overrightarrow{M}$ and the field $\overrightarrow{B'}$.

The metallic implant is assumed to be an isotropic linear paramagnetic or diamagnetic material. We will assume, this is our main assumption, the magnetization $\overrightarrow{M}$ to be parallel to the applied field, that is

$$\overrightarrow{M} = \frac{\chi_m}{\mu_0} \overrightarrow{B_0}, \tag{6}$$

where χ_m is the magnetic susceptibility of the magnetic material. The relation (6) is justified since for non ferromagnetic material the order of magnitude for the induced field is up to 10^{-4} times the order of magnitude of $\overrightarrow{B_0}$, see [14] and [15] for details in MRI applications.

The assumption (6), that is the magnetization is uniform in Ω, is crucial in our study. Indeed for ferromagnetic material constitutive laws are non linear and the mathematical model is different. Studies for problems involving ferromagnetic material are numerous in the literature, with regard to their mathematical analysis, see [11] for instance, or to their numerical resolution, see [16], [12]. The reason why we have restricted our study to paramagnetic material is that patients bearing ferromagnetic implants are usually kept off from MRI.

The interface condition in (5) with the assumption (6) takes the form

$$[\overrightarrow{B'} \wedge \overrightarrow{n}] = \overrightarrow{j_\Sigma} \quad \text{where} \quad \overrightarrow{j_\Sigma} = \chi_m \; (\overrightarrow{B_0} \wedge \overrightarrow{n}). \tag{7}$$

Remark 2.1 We can check that $\operatorname{div}_\Sigma \overrightarrow{j_\Sigma} = 0$ so that $\overrightarrow{j_\Sigma}$ can be interpreted as a fictitious current density over the surface Σ, see [4]. Then problem (5) with the interface condition (7) can be interpreted as a standard magnetostatic problem for surface currents. Variational formulations for such problems are given in [9]. However, a finite element approach based on it is not satisfying at all. $\diamond$

Our approach to deal with (5) and (7) consists in introducing the scalar magnetic potential and using standard results from the potential theory to deduce (see [6], [4] for details) that the solution $\overrightarrow{B'}$ of (5) and (7) can be expressed as

$$\overrightarrow{B}'(P) = \mu_0 \overrightarrow{M} + \frac{\mu_0}{4\pi} \int_\Sigma \left(\overrightarrow{M} \cdot \frac{\overrightarrow{r}}{r^3} \right) \; \overrightarrow{n}(Q) \; \mathrm{d}\sigma(Q) \tag{8}$$

for $P \in \Omega$, and

$$\overrightarrow{B}'(P) = \frac{\mu_0}{4\pi} \int_\Sigma \left(\overrightarrow{M} \cdot \frac{\overrightarrow{r}}{r^3} \right) \; \overrightarrow{n}(Q) \; \mathrm{d}\sigma(Q) \tag{9}$$

for P in the exterior domain Ω', where $\overrightarrow{r} = P - Q$ and the magnetization $\overrightarrow{M}$ is given by (6). So we have reduced our problem to quadrature formulae. On one hand, (8) and (9) give an explicit representation for $\overrightarrow{B'}$, no system needs to be solved. On the other hand, the integration bears only on the interface Σ and not on the whole domain Ω.

Therefore the computation of the magnetic flux induction $\overrightarrow{B'}$ is reduced to the evaluation of the integrals

$$\mathcal{B}(P) = \int_\Sigma \left(\overrightarrow{M} \cdot \frac{\overrightarrow{r}}{r^3} \right) \; \overrightarrow{n}(Q) \; \mathrm{d}\sigma(Q). \tag{10}$$

To compute it we introduce a triangulation of the interface Σ made up of a finite union of flat and curved triangles. Let T_h^1 denote the set of all flat triangles and T_h^2 the set of all curved triangles. We have the relation

$$\Sigma = \left(\bigcup_{K \in T_h^1} K \right) \cup \left(\bigcup_{K \in T_h^2} K \right). \tag{11}$$

Therefore the integral in (10) can be split into two terms in the following way

$$\begin{aligned} \mathcal{B}(P) = & \sum_{K \in T_h^1} \int_K \left(\overrightarrow{M} \cdot \frac{\overrightarrow{r}}{r^3} \right) \; \overrightarrow{n}(Q) \;\; \mathrm{d}\sigma(Q) \\ & + \sum_{K \in T_h^2} \int_K \left(\overrightarrow{M} \cdot \frac{\overrightarrow{r}}{r^3} \right) \; \overrightarrow{n}(Q) \; \mathrm{d}\sigma(Q). \end{aligned} \tag{12}$$

These two terms are evaluated using two distinct methods.

For flat triangles, the normal vector $\overrightarrow{n}$ to Σ is constant on each triangle. Since the magnetization $\overrightarrow{M}$ is uniform in Ω we can write the first sum in (12) as

$$S_1(P) = \sum_{K \in T_h^1} \left(\overrightarrow{M} \cdot \int_K \frac{\overrightarrow{r}}{r^3} \; \mathrm{d}\sigma(Q) \right) \overrightarrow{n} \; . \tag{13}$$

Consequently, S_1 is obtained by computing the integrals

$$\int_K \frac{\overrightarrow{r}}{r^3} \; \mathrm{d}\sigma(Q) \quad \text{for} K \in T_h^1. \tag{14}$$

These last integrals can be calculated exactly, see for instance [5], [17], [10] for the resulting formulae. This is of great practical importance since for the flat parts of the interface no numerical scheme is needed. Moreover for any polyhedral object, the induced magnetic field can be calculated exactly. In particular for flat panels, the precision in the computation of the integrals in (13) does not depend on the size of the triangles used to mesh the panels. In fact one should use triangles with a maximal size to reduce the number of integrals to evaluate.

So our work concerns now the computation of the second sum in (12), that is to say the computation of the integral (10) over the curved panels of the boundary. We will first present the method and then give an error analysis.

3 Computation of the integral over the curved panels

3.1 Approximation of the surface

We consider the case where the interface Σ is made of curved panels. As discussed in [1], we assume that the surface Σ can be written as $\Sigma = \Sigma_1 \cup \Sigma_2 \cup \cdots \cup \Sigma_J$ where each Σ_j is a closed smooth surface in $\mathbb{R}^3$. A pair of sub-surface can intersect only along a common portion of edges. We also assume each Σ_j has a parametrization six time continuously differentiable, i.e. there is a mapping $F_j : D_j \longmapsto \Sigma_j$, where D_j is a polygonal domain in the plane and $F_j \in C^6(D_j)$.

Since the D_j domains are polygonal, they can be written as a union of triangles and without loss of generality we will assume that the D_j domains are triangles. To each D_j we associate a triangulation $\widehat{T}_h^j$, $\widehat{T}_h^j = \{\widehat{K}_k^j, 1 \leq k \leq N^j\}$. Here the parameter h represents the mesh size of the triangulation, that is

$$h = \max_{1 \leq k \leq N^j} \mathrm{diam}(\widehat{K}_k^j) \quad \text{where} \quad \mathrm{diam}(\widehat{K}_k^j) = \max_{P,Q \in \widehat{K}_k^j} |P - Q|,$$

with $|\cdot|$ being the usual euclidian norm.

Then a triangulation of Σ can be constructed via a triangulation of each panel Σ_j, the image of $\widehat{T}_h^j$ through the parametrization F_j. More precisely let T_h^j be the image of the triangulation $\widehat{T}_h^j$ of Σ_j by the mapping F_j and let K denote a generic element of that triangulation. The corresponding triangle in $\widehat{T}_h^j$ is denoted by $\widehat{K}$ whose vertices are $\widehat{v}_1, \widehat{v}_2$, and $\widehat{v}_3$. We shall also use the reference element σ, the unit simplex in the plane, $\sigma = \{(s,t) \in [0,1]^2 \setminus 0 \leq s + t \leq 1\}$ and the set $\{\rho_i, i = 1, \cdots, 6\}$ of its vertices and its midpoints numbered according to Figure 1. We define now the mapping $m_K : (s,t) \in \sigma \mapsto m_K(s,t) \in \mathbb{R}^3$, by

$$m_K(s,t) = F_j(u \; \widehat{v}_1 + t \; \widehat{v}_2 + s \; \widehat{v}_3), \qquad u = 1 - s - t; \tag{15}$$

then the curved triangular element K is precisely the image of σ by the mapping m_K, see Figure 1 for a complete picture. We will also use the following notation, for $(s,t) \in \sigma$,

$$m_K(s,t) = \begin{pmatrix} x_K^1(s,t) \\ x_K^2(s,t) \\ x_K^3(s,t) \end{pmatrix}. \tag{16}$$

In fact to carry out the computations over a surface Σ_j we need to know explicitly the mapping F_j or the m_K ones. Usually in effective computations, they are not known explicitly, only points of the surface are used. Then it is convenient to approximate Σ by using a piecewise quadratic interpolation of the surface. The approximate surface $\Sigma_{j,h}$ is then composed of elements $\widetilde{K}$ quadratic approximations of the elements K. If $\{L_i; i = 1, \ldots, 6\}$ is the set of the six basis functions associated to the nodes $\rho_j, j = 1, \ldots, 6$, for quadratic interpolation over σ, then $\widetilde{K}$ is the image of σ by $\widetilde{m}_K$ where

$$\widetilde{m}_K(s,t) = \sum_{i=1}^{6} m_K(\rho_i)\ L_i(s,t) = \begin{pmatrix} \sum_{i=1}^6 x_K^1(\rho_i)\ L_i(s,t) \\ \sum_{i=1}^6 x_K^2(\rho_i)\ L_i(s,t) \\ \sum_{i=1}^6 x_K^1(\rho_i)\ L_i(s,t) \end{pmatrix} = \begin{pmatrix} \tilde{x}_K^1(s,t) \\ \tilde{x}_K^2(s,t) \\ \tilde{x}_K^3(s,t) \end{pmatrix}. \tag{17}$$

Clearly each component of $\widetilde{m}_K(s,t)$ is quadratic in (s,t). In the sequel the index j will be omitted when not necessary.

3.2 Approximation of the integral

With the approximation of the surface given above we are in position to present the actual quadrature formulae used to compute the surface integral (10). We note Φ the function given by

$$\Phi(P,Q) = \overrightarrow{M}.\frac{\overrightarrow{r}}{r^3}(P,Q). \tag{18}$$

Then the integral in (10) reads

$$\begin{aligned} \mathcal{B}(P) &= \int_\Sigma \Phi(P,Q)\ \overrightarrow{n}(Q)\ \mathrm{d}\sigma(Q) \\ &= \sum_{j=1}^{J} \int_{\Sigma_j} \Phi(P,Q)\ \overrightarrow{n}(Q)\ \mathrm{d}\sigma(Q). \end{aligned} \tag{19}$$

For ease of exposition we will consider the integral over one panel Σ_j and we will omit the index j. Therefore our analysis will be carried out for a surface integral $\mathcal{B}(P)$ given by

$$\begin{aligned} \mathcal{B}(P)\ \ (\equiv \mathcal{B}_j(P)\ ) &= \sum_{\widehat{K} \in \widehat{T}_h} \int_{F(\widehat{K})} \Phi(P,Q)\ \overrightarrow{n}(Q)\ \mathrm{d}\sigma(Q) \\ &= \sum_{K \in T_h} \int_\sigma \Phi(P, m_K(s,t))\ \overrightarrow{n}(m_K(s,t))\ J(s,t)\ \mathrm{d}s\ \mathrm{d}t, \end{aligned} \tag{20}$$

with $J(s,t) = |\ \partial_s m_K(s,t) \wedge \partial_t m_K(s,t)\ |$. The unit normal vector to the surface Σ is given by

$$\overrightarrow{n}(m_K(s,t)) \equiv n(s,t) = \frac{\partial_s m_K(s,t) \wedge \partial_t m_K(s,t)}{|\ \partial_s m_K(s,t) \wedge \partial_t m_K(s,t)\ |}. \tag{21}$$

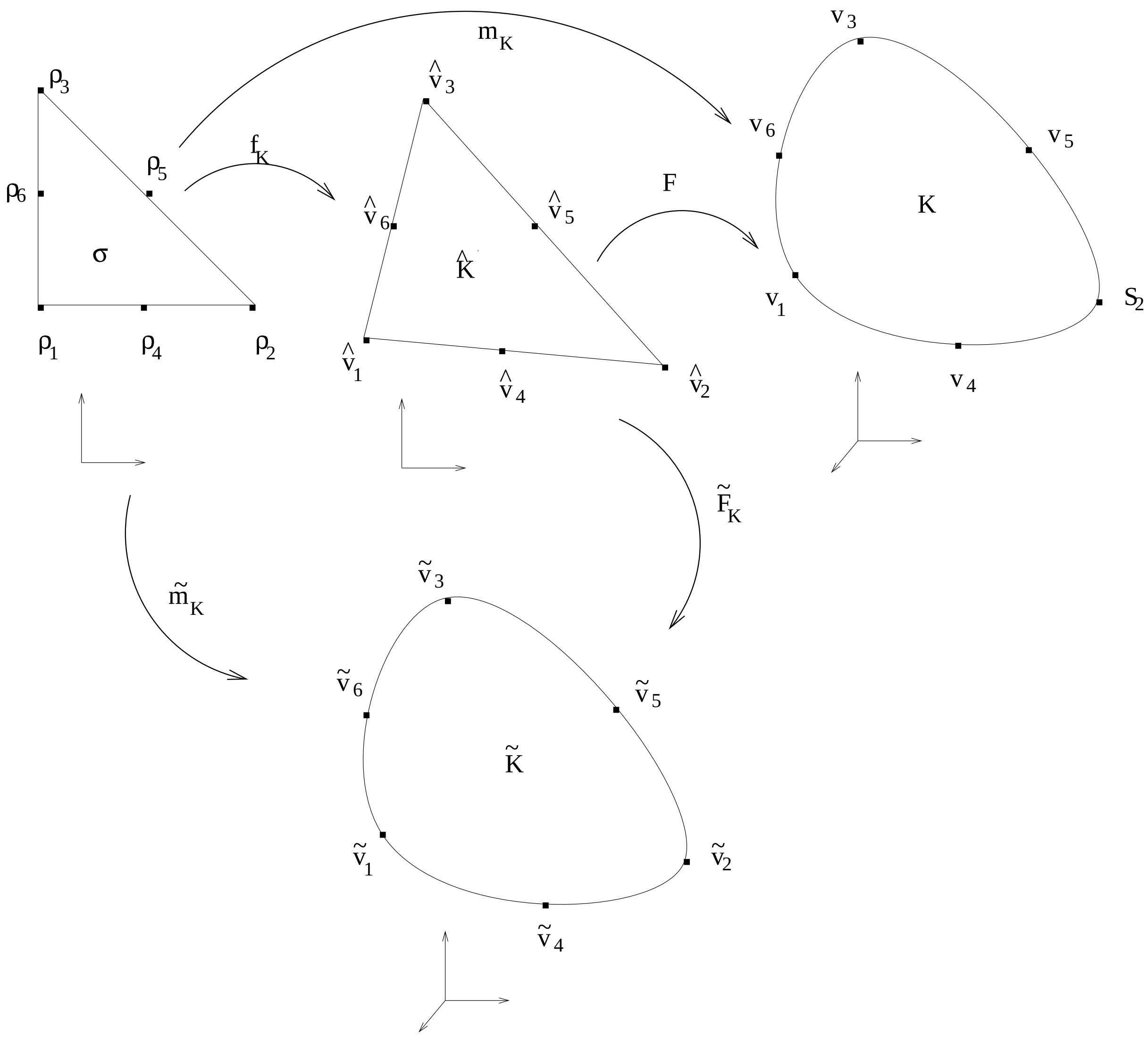

Figure 1: The global picture of mappings

As mentioned before the mappings m_K are not known explicitly, but the $\widetilde{m}_K$ ones are. That is why we will consider an approximation of $\mathcal{B}$ in (20) given by

$$\mathcal{B}_h(P) = \sum_{K \in T_h} \int_\sigma \Phi(P, \widetilde{m}_K(s,t))\ \widetilde{n}(s,t)\ \widetilde{J}(s,t)\ \mathrm{d}s\ \mathrm{d}t, \tag{22}$$

with $\tilde{J}(s,t) = \mid \partial_s \widetilde{m}_K(s,t) \wedge \partial_t \widetilde{m}_K(s,t) \mid$ and the approximation of the normal

$$\widetilde{n}(s,t) = \frac{\partial_s \widetilde{m}_K(s,t) \wedge \partial_t \widetilde{m}_K(s,t)}{\mid \partial_s \widetilde{m}_K(s,t) \wedge \partial_t \widetilde{m}_K(s,t) \mid}. \tag{23}$$

Note that $\mathcal{B}_h(P)$ can be rewritten as

$$\mathcal{B}_h(P) = \sum_{\widetilde{K} \in \widetilde{T}_h} \int_{\widetilde{K}} \Phi(P,Q)\ \widetilde{n}(Q)\ \ \mathrm{d}\sigma(Q) = \int_{\Sigma_h} \Phi(P,Q)\ \widetilde{n}(Q)\ \ \mathrm{d}\sigma(Q). \tag{24}$$

Now to numerically compute the integrals in (22) the standard approach is to use a quadrature rule over the unit simplex σ,

$$\int_\sigma f(s,t)\ \ \mathrm{d}s\ \mathrm{d}t \approx \sum_{j=1}^{\mu_d} \omega_j f(u_j) \tag{25}$$

where the $\omega_j \in \mathbb{R}$ are the quadrature weights and $u_j = (s_j, t_j) \in \sigma$ the quadrature nodes. The quadrature formula we will generally use is the $3 - points$ rule

$$\int_\sigma f(s,t)\ \ \mathrm{d}s\ \mathrm{d}t \approx \frac{1}{6} \sum_{j=4}^{6} f(\rho_j). \tag{26}$$

This formula is exact for polynomials of degree up to 2. Then the integral in (24) is approximated by the expression

$$\mathcal{B}_h^\mu(P) = \sum_{K \in T_h} \sum_{j=1}^{\mu_d} \omega_j \Phi(P, \widetilde{m}_K(u_j))\ (\partial_s \widetilde{m}_K(u_j) \wedge \partial_t \widetilde{m}_K(u_j)), \tag{27}$$

which represents precisely what is computed.

We point out that the integrand in (22) is always analytical since $P \notin \Sigma$. However, it is increasingly peaked as the distance from P to Σ decreases. Such integrals are known as quasi-singular integrals. A special attention has to be paid for points P closed to the boundary Σ. There are two ways to handle such integrals, see [13]. In the first one we do a change of variables to reduce the singular behavior of the integrand. The second one consists in increasing the number of quadrature nodes, either by changing the quadrature rule or by subdividing the integration domain. Here we use a method introduced in [2] that consists in subdividing the reference element σ and then use the quadrature rule $T2 : 5.1$ of [18],

$$\begin{aligned} \int_\sigma f(s,t)\ \ \mathrm{d}s\ \mathrm{d}t\ \ &\approx\ \ \frac{9}{80} f(\frac{1}{3}, \frac{1}{3}) + B\left\{f(\alpha,\alpha) + f(\alpha,\beta) + f(\beta,\alpha)\right\} \\ &\quad + C\left\{f(\gamma,\gamma) + f(\gamma,\zeta) + f(\zeta,\zeta)\right\}, \end{aligned} \tag{28}$$

with

$$\begin{cases} \alpha = \dfrac{6-\sqrt{5}}{21} \quad , \quad \beta = \dfrac{9+2\sqrt{15}}{21} \quad , \quad \gamma = \dfrac{6+\sqrt{5}}{21} \\[2ex] \zeta = \dfrac{9-2\sqrt{15}}{21} \quad , \quad B = \dfrac{155-\sqrt{15}}{2400} \quad , \quad C = \dfrac{155+\sqrt{15}}{2400}, \end{cases}$$

on each sub-element. The number of subdivisions to use depends on the distance from P to the triangle. As the distance between P and K increases, the number of subdivisions of σ decreases, eventually reaching an integration over σ with no subdivision needed and where the use of the $3-points$ rule (26) is accurate enough. It appears from numerical experiments, see Section 5, that for a point P at a distance exceeding $3h$, h being the mesh size, the $3-points$ rule (26) is adequate.

Let us mention that if the surface Σ is approximated via a piecewise linear approximation, then the integrals in (22) can be evaluated analytically. However, a piecewise linear approximation would not lead to results accurate enough, due to the presence in the integrand of the normal vector.

4 Error estimates

Let $E(P)$ denote the error between the exact integral $\mathcal{B}(P)$ in (20) and its approximation $\mathcal{B}_h(P)$ in (22); $E(P) = \mathcal{B}(P) - \mathcal{B}_h(P)$ for $P \in \mathbb{R}^3$. Our goal is to carefully overestimate $E(P)$. In our study we are using tools introduced in [3] in the framework of piecewise polynomial collocation for integral equations on surfaces in $\mathbb{R}^3$. Here the integrals, although having different integrands, can be handled in a similar way.

First we shall study the error $E(P)$, only due to the approximation of the surface Σ, for a point P not in Σ fixed. We prove that the order of convergence is h^4, which is higher than the convergence rate h^3 that would be expected based on the underlying interpolation error estimates. Then we will study the error when using quadrature formulae. The argumentation is somewhat technical, we will leave the obvious details to the reader. In the following, we will give up reference to index K when not necessary and refer to the derivation with respect to the variable s by ∂_s or by the subscript s. We also set $\Phi_P(.) = \Phi(P,.)$.

We decompose the error $E(P)$

$$\begin{aligned} E(P) \quad = \quad & \sum_{K\in T_h} \int_\sigma \{ \ \Phi_P(m_K(s,t)) \ \ (\partial_s m_K(s,t) \wedge \partial_t m_K(s,t)) - \\ & \Phi_P(\widetilde{m}_K(s,t)) \, (\partial_s \widetilde{m}_K(s,t) \wedge \partial_t \widetilde{m}_K(s,t)) \ \} \ \ \mathrm{d}s \ \mathrm{d}t \end{aligned} \tag{29}$$

into two terms,

$$E(P) = E_1(P) + E_2(P), \tag{30}$$

where

$$
\begin{cases}
E_1(P) &= \displaystyle\sum_{K\in T_h} \int_\sigma \Phi_P(m_K(s,t)) \\
& \qquad \times \{\partial_s m_K(s,t)\wedge \partial_t m_K(s,t) - \partial_s \widetilde{m}_K(s,t)\wedge \partial_t \widetilde{m}_K(s,t)\} \;\; \mathrm{d}s \; \mathrm{d}t, \\
E_2(P) &= \displaystyle\sum_{K\in T_h} \int_\sigma \{\Phi_P(m_K(s,t)) - \Phi_P(\widetilde{m}_K(s,t))\} \\
& \qquad \times (\partial_s \widetilde{m}_K(s,t)\wedge \partial_t \widetilde{m}_K(s,t)) \;\; \mathrm{d}s \; \mathrm{d}t.
\end{cases}
\tag{31}
$$

The first term gives the error when approximating the normal to the surface Σ and the second one the error when computing the integrand on the approximated surface Σ_h.

4.1 Error when approximating the normal

We start with an estimate on each triangle between the normal to the surface and the normal to the approximated surface. More precisely our result is the following.

Lemma 4.1 *For each triangle $K \in T_h$ and $\forall (s,t) \in \sigma$,*

$$\mid \partial_s m_K(s,t)\wedge \partial_t m_K(s,t) - \partial_s \widetilde{m}_K(s,t)\wedge \partial_t \widetilde{m}_K(s,t) \mid = O(h^4).$$

Proof We set $e_{n,K}(s,t) = \partial_s m_K(s,t)\wedge \partial_t m_K(s,t) - \partial_s \widetilde{m}_K(s,t)\wedge \partial_t \widetilde{m}_K(s,t)$. Componentwise we have with the notations (16), (17),

$$
e_{n,K}(s,t) = \begin{pmatrix}
x_s^2(s,t)x_t^3(s,t) - x_s^3(s,t)x_t^2(s,t) - \tilde{x}_s^2(s,t)\tilde{x}_t^3(s,t) + \tilde{x}_s^3(s,t)\tilde{x}_t^2(s,t) \\
x_s^3(s,t)x_t^1(s,t) - x_s^1(s,t)x_t^3(s,t) - \tilde{x}_s^3(s,t)\tilde{x}_t^1(s,t) + \tilde{x}_s^1(s,t)\tilde{x}_t^3(s,t) \\
x_s^1(s,t)x_t^2(s,t) - x_s^2(s,t)x_t^1(s,t) - \tilde{x}_s^1(s,t)\tilde{x}_t^2(s,t) + \tilde{x}_s^2(s,t)\tilde{x}_t^1(s,t)
\end{pmatrix}.
$$

To get estimates for $e_{n,K}(s,t)$, we need to develop the functions $x^i(s,t)$ and $\tilde{x}^i(s,t)$. The Taylor expansion of $x^i(s,t)$ in a neighborhood of the origin gives

$$
\begin{aligned}
x^i(s,t) &= x^i(0,0) + (s\frac{\partial}{\partial s} + t\frac{\partial}{\partial t})x^i(0,0) + \frac{1}{2}(s\frac{\partial}{\partial s} + t\frac{\partial}{\partial t})^2 x^i(0,0) \\
&\quad + \frac{1}{6}(s\frac{\partial}{\partial s} + t\frac{\partial}{\partial t})^3 x^i(0,0) + \frac{1}{24}(s\frac{\partial}{\partial s} + t\frac{\partial}{\partial t})^4 x^i(0,0) + O(h^5).
\end{aligned}
\tag{32}
$$

Then the function $\tilde{x}^i(s,t)$ in (17) admits the development

$$
\begin{aligned}
\tilde{x}^i(s,t) &= \sum_{j=1}^{6} \Big(x^i(0,0) + (s_j\frac{\partial}{\partial s} + t_j\frac{\partial}{\partial t})x^i(0,0) + \frac{1}{2}(s_j\frac{\partial}{\partial s} + t_j\frac{\partial}{\partial t})^2 x^i(0,0) \\
&+ \frac{1}{6}(s_j\frac{\partial}{\partial s} + t_j\frac{\partial}{\partial t})^3 x^i(0,0) + \frac{1}{24}(s_j\frac{\partial}{\partial s} + t_j\frac{\partial}{\partial t})^4 x^i(0,0) + O(h^5)\Big) \;\; L_j(s,t).
\end{aligned}
\tag{33}
$$

It is not difficult to check that the basis functions $L_j(s,t)$ satisfy to

$$
\begin{aligned}
&\sum_{j=1}^{6} L_j(s,t) = 1, \\
&\sum_{j=1}^{6} s_j \; L_j(s,t) = s, \quad \sum_{j=1}^{6} t_j \; L_j(s,t) = t, \\
&\sum_{j=1}^{6} s_j^2 \; L_j(s,t) = s^2, \quad \sum_{j=1}^{6} s_j \; t_j \; L_j(s,t) = s \; t, \quad \sum_{j=1}^{6} t_j^2 \; L_j(s,t) = t^2.
\end{aligned}
$$

We make the difference $x^i(s,t) - \tilde{x}^i(s,t)$ in (32) and (33) and use the relations above to finally obtain

$$x^i(s,t) = \tilde{x}^i(s,t) + H^i(s,t) + G^i(s,t) + O(h^5), \tag{34}$$

where

$$H^i(s,t) = \frac{1}{6}\left\{(s\frac{\partial}{\partial s} + t\frac{\partial}{\partial t})^3 x^i(0,0) - \sum_{j=1}^{6}\left\{(s_j\frac{\partial}{\partial s} + t_j\frac{\partial}{\partial t})^3 x^i(0,0)\right\} L_j(s,t)\right\}, \tag{35}$$

$$G^i(s,t) = \frac{1}{24}\left\{(s\frac{\partial}{\partial s} + t\frac{\partial}{\partial t})^4 x^i(0,0) - \sum_{j=1}^{6}\left\{(s_j\frac{\partial}{\partial s} + t_j\frac{\partial}{\partial t})^4 x^i(0,0)\right\} L_j(s,t)\right\}. \tag{36}$$

Notice that

$$H^i(s,t) = O(h^3) \quad \text{and} \quad G^i(s,t) = O(h^4), \tag{37}$$

since the derivatives of x^i with respect to (s,t) give rise to formula involving $\hat{v}_2 - \hat{v}_1$ and $\hat{v}_3 - \hat{v}_1$. For example

$$\begin{aligned} \partial_s x^i(s,t) &= \nabla F^i(u\ \hat{v}_1 + t\ \hat{v}_2 + s\ \hat{v}_3) \cdot (\hat{v}_3 - \hat{v}_1) = O(h), & (38)\\ \partial_t x^i(s,t) &= \nabla F^i(u\ \hat{v}_1 + t\ \hat{v}_2 + s\ \hat{v}_3) \cdot (\hat{v}_2 - \hat{v}_1) = O(h); & (39) \end{aligned}$$

the generalization for derivatives of any order is immediate.

We use equation (34) to express $e_{n,K}(s,t)$ as a function of the derivatives of x^i, H^i, and G^i. For instance the first component of $e_{n,K}(s,t)$ becomes

$$\begin{aligned} e^1_{n,K}(s,t) &= x^2_s(s,t)(H^3_t(s,t) + G^3_t(s,t)) + x^3_t(s,t)(H^2_s(s,t) + G^2_s(s,t)) \\ &- x^3_s(s,t)(H^2_t(s,t) + G^2_t(s,t)) - x^2_t(s,t)(H^3_s(s,t) + G^3_s(s,t)) \\ &+ (H^3_s(s,t) + G^3_s(s,t))(H^2_t(s,t) + G^2_t(s,t)) \\ &- (H^2_s(s,t) + G^2_s(s,t))(H^3_t(s,t) + G^3_t(s,t)) + O(h^6). \end{aligned} \tag{40}$$

Then, a Taylor expansion of x^i_s, x^i_t at $(0,0)$ leads to

$$\begin{aligned} e^1_{n,K}(s,t) &= \{x^2_s(0,0) + s\ x^2_{ss}(0,0) + t\ x^2_{st}(0,0)\}\{H^3_t(s,t) + G^3_t(s,t)\} \\ &+ \{x^3_t(0,0) + s\ x^3_{st}(0,0) + t\ x^3_{tt}(0,0)\}\{H^2_s(s,t) + G^2_s(s,t)\} \\ &- \{x^3_s(0,0) + s\ x^3_{ss}(0,0) + t\ x^3_{st}(0,0)\}\{H^2_t(s,t) + G^2_t(s,t)\} \\ &- \{x^2_t(0,0) + s\ x^2_{st}(0,0) + t\ x^2_{tt}(0,0)\}\{H^3_s(s,t) + G^3_s(s,t)\} + O(h^6) \end{aligned} \tag{41}$$

Finally the i^{th} component of the error $e_{n,K}(s,t)$ can be expressed as

$$e^i_{n,K}(s,t) = E^i_4(s,t) + E^i_5(s,t) + O(h^6) \tag{42}$$

where

$$\begin{aligned} E^i_4(s,t) &= x^{i+1}_s(0,0)H^{i+2}_t(s,t) + x^{i+2}_t(0,0)H^{i+1}_s(s,t) \\ &- x^{i+2}_s(0,0)H^{i+1}_t(s,t) - x^{i+1}_t(0,0)H^{i+2}_s(s,t) \end{aligned} \tag{43}$$

is a collection of term which are of order 4 in h and

$$\begin{array}{rcl} E_5^i(s,t) & = & x_s^{i+1}(0,0)G_t^{i+2}(s,t) + x_t^{i+2}(0,0)G_s^{i+1}(s,t) \\ & - & x_s^{i+2}(0,0)G_s^{i+1}(s,t) - x_t^{i+1}(0,0)G_s^{i+2}(s,t) \\ & + & \{s\ x_{ss}^{i+1}(0,0) + t\ x_{st}^{i+1}(0,0)\}\{H_t^{i+2}(s,t) + G_t^{i+2}(s,t)\} \\ & + & \{s\ x_{st}^{i+2}(0,0) + t\ x_{tt}^{i+2}(0,0)\}\{H_s^{i+1}(s,t) + G_s^{i+1}(s,t)\} \\ & - & \{s\ x_{ss}^{i+2}(0,0) + t\ x_{st}^{i+2}(0,0)\}\{H_t^{i+1}(s,t) + G_t^{i+1}(s,t)\} \\ & - & \{s\ x_{st}^{i+1}(0,0) + t\ x_{tt}^{i+1}(0,0)\}\{H_s^{i+2}(s,t) + G_s^{i+2}(s,t)\} \end{array} \tag{44}$$

is a collection of term which are of order 5 in h. $\diamond$

4.2 Some intermediate technical results

Lemma 4.2 *For all $i \in \{1,2,3\}$, we have for E_4^i given in (43)*

$$\int_\sigma E_4^i(s,t)\ \mathrm{d}s\ \mathrm{d}t = 0. \tag{45}$$

Proof With the expression (43) the lemma is proved once we prove for $i = 1,2,3$

$$\int_\sigma \frac{\partial}{\partial s} H^i(s,t)\ \mathrm{d}s\ \mathrm{d}t = 0 \quad \text{and} \quad \int_\sigma \frac{\partial}{\partial t} H^i(s,t)\ \mathrm{d}s\ \mathrm{d}t = 0. \tag{46}$$

We know the particular form of $H^i(s,t)$ in (35). Then (46) is a consequence of the following result. Let f be the function defined by $f(s,t) = c_1 s^3 + c_2 s^2 t + c_3 s t^2 + c_4 t^3$, where $c_1, c_2, c_3, c_4 \in \mathbb{R}$. The quadratic interpolant of f is given by $\Pi(s,t) = \sum_{i=1}^6 f(\rho_i) L_i(s,t)$. Then we can check by a straightforward calculation that

$$\int_\sigma \frac{\partial}{\partial s}(f(s,t) - \Pi(s,t))\ \mathrm{d}s\ \mathrm{d}t = 0 = \int_\sigma \frac{\partial}{\partial t}(f(s,t) - \Pi(s,t))\ \mathrm{d}s\ \mathrm{d}t. \tag{47}$$

$\diamond$

The next lemma is the key-point of our error analysis. It uses the notion of *pair of symmetric triangles* that was introduced by D. Chien [7] for his error analysis of a collocation method for some integral equations. We call pair of symmetric triangles, see Figure 2, two triangles $\widehat{K}_1, \widehat{K}_2 \in \widehat{T}_h$ with vertices $\widehat{v}_1, \widehat{v}_2, \widehat{v}_3$ and $\widehat{v}_1, \widehat{v}_4, \widehat{v}_5$ respectively, having the following property

$$\left\{ \begin{array}{rcl} \widehat{v}_1 - \widehat{v}_2 & = & -\ (\widehat{v}_1 - \widehat{v}_4), \\ \widehat{v}_1 - \widehat{v}_3 & = & -\ (\widehat{v}_1 - \widehat{v}_5). \end{array} \right. \tag{48}$$

Lemma 4.3 *Let D be a right-angled, isosceles triangle. Let T_h be a triangulation of D composed of N^2 right-angled, isosceles triangles. Then if N is odd, there exists $\frac{1}{2}\left(N^2 - N\right)$ pairs of symmetric triangles and N unmatched triangles. If N is even, there exists $\frac{1}{2}(N^2 - 3N + 2)$ pairs of symmetric triangles and $3N - 2$ unmatched triangles.*

Proof The proof of the lemma is elementary. The basic idea consists in considering the pattern shown in Figure 2 made of 3 pairs of symmetric triangles and reproducing this pattern in the triangulation of D a maximum number of times. Counting the number of remaining triangles in the triangulation gives the result. $\diamond$

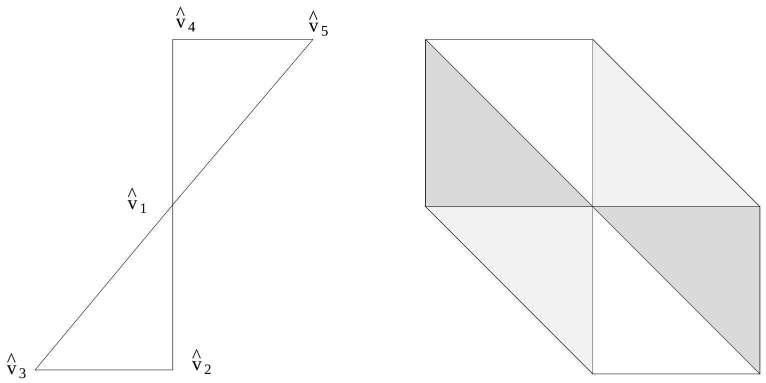

Figure 2: A pair of symmetric triangles and the pattern made of 3 such pairs.

Due to pairs of symmetric triangles cancellation will occur among the terms contributing to the local error.

Lemma 4.4 *Let $\widehat{K}_1$, $\widehat{K}_2$ be a pair of symmetric triangles and K_1, K_2 be their images in T_h, then*

$$E_4^i(s,t)|_{K_1} = E_4^i(s,t)|_{K_2} \tag{49}$$

and

$$E_5^i(s,t)|_{K_1} + E_5^i(s,t)|_{K_2} = O(h^6). \tag{50}$$

Proof Let $\widehat{v}_1, \widehat{v}_2, \widehat{v}_3$ and $\widehat{v}_1, \widehat{v}_4, \widehat{v}_5$ be the vertices of the two triangles $\widehat{K}_1$ and $\widehat{K}_2$ as in Figure 2. Let (a_i, b_i) denote the coordinates of $\widehat{v}_i$. We have

$$\begin{array}{rclcrcl} a_1 - a_2 & = & a_4 - a_1, & \quad & b_1 - b_2 & = & b_4 - b_1, \\ a_1 - a_3 & = & a_5 - a_1, & & b_1 - b_3 & = & b_5 - b_1. \end{array} \tag{51}$$

Then $\forall i \in \{1,2,3\}$

$$\begin{array}{rcl} \partial_s x^i_{K_1}(0,0) & = & (a_3 - a_1)\ \partial_1 F^i(a_1,b_1) + (b_3 - b_1)\ \partial_2 F^i(a_1,b_1) \\ & = & -(a_5 - a_1)\ \partial_1 F^i(a_1,b_1) - (b_5 - b_1)\ \partial_2 F^i(a_1,b_1) = -\partial_s x^i_{K_2}(0,0). \end{array} \tag{52}$$

A similar development leads to $\partial_t x^i_{K_1}(0,0) = -\partial_t x^i_{K_2}(0,0)$ and

$$\left\{ \begin{array}{rcrl} \partial^2_\alpha\ x^i_{K_1}(0,0) & = & & \partial^2_\alpha\ x^i_{K_2}(0,0), \quad \forall \alpha \in \{ss, st, tt\}, \\ \partial^3_\alpha\ x^i_{K_1}(0,0) & = & - & \partial^3_\alpha\ x^i_{K_2}(0,0), \quad \forall \alpha \in \{sss, sst, stt, ttt\}, \\ \partial^4_\alpha\ x^i_{K_1}(0,0) & = & & \partial^4_\alpha\ x^i_{K_2}(0,0), \quad \forall \alpha \in \{ssss, ssst, sstt, sttt, tttt\}. \end{array} \right. \tag{53}$$

This last result is used in (35) and (36) combined with (43) and (44) to check (49), (50). $\diamond$

4.3 Error estimate for $\mathcal{B}(P) - \mathcal{B}_h(P)$ with P fixed not in Σ

We will assume now that the triangulation $\widehat{T}_h$ of the domain D is structured so that it is composed of $O(N^2)$ pairs of symmetric triangles and $O(N)$ pairs of unmatched triangles. Such a triangulation exists, only to transform the mesh so as to apply Lemma 4.3.

Lemma 4.5 *Let P be a point not in Σ. Then the error $E_1(P)$ defined in (31) behaves in $O(h^4)$,*

$$E_1(P) = O(h^4).$$

Proof The error on the element K is

$$e_{1,K}(P) = \int_\sigma \Phi_P(m_K(s,t)) \left\{\partial_s m_K(s,t) \wedge \partial_t m_K(s,t) - \partial_s \widetilde{m}_K(s,t) \wedge \partial_t \widetilde{m}_K(s,t)\right\} \text{ d}s \text{ d}t. \tag{54}$$

The Taylor expansion of $\Phi_P(m_K(s,t))$ at $(s,t)=(0,0)$ leads to

$$\begin{aligned}\Phi_P(m_K(s,t)) &= \Phi_P(m_K(0,0)) + s\ \nabla\Phi_P(m_K(0,0)) \cdot \partial_s m_K(0,0) \\ &\quad + t\ \nabla\Phi_P(m_K(0,0)) \cdot \partial_t m_K(0,0) + O(h^2).\end{aligned} \tag{55}$$

Using Lemmas 4.1 and 4.2 we get the expression for the i^{th} component of $e_{1,K}$,

$$\begin{aligned}e^i_{1,K}(P) &= \int_\sigma \Phi_P(m_K(0,0))\ E^i_5(s,t) \text{ d}s \text{ d}t + \int_\sigma \{s\ \nabla\Phi_P(m_K(0,0)) \cdot \partial_s m_K(0,0) \\ &\quad + t\ \nabla\Phi_P(m_K(0,0)) \cdot \partial_t m_K(0,0)\}\, E^i_4(s,t) \text{ d}s \text{ d}t + O(h^6).\end{aligned} \tag{56}$$

Therefore the local error $e_{1,K}$ over a triangle K is of order h^5 and summing over the N^2 triangles of the triangulation would lead to a global error E_1 of order h^3. To improve the estimate we consider a pair of symmetric triangles $\widehat{K}_1$ and $\widehat{K}_2$ and their corresponding images K_1 and K_2 in T_h. By using the relations (53), it can be easily verified that

$$\begin{aligned}&s\ \nabla\Phi_P(m_{K_1}(0,0)) \cdot \partial_s m_{K_1}(0,0) + t\ \nabla\Phi_P(m_{K_1}(0,0)) \cdot \partial_t m_{K_1}(0,0) \\ =\ &-s\ \nabla\Phi_P(m_{K_2}(0,0)) \cdot \partial_s m_{K_2}(0,0) - t\ \nabla\Phi_P(m_{K_2}(0,0)) \cdot \partial_t m_{K_2}(0,0).\end{aligned} \tag{57}$$

It then follows from Lemma 4.4 that

$$e^i_{1,K_1} + e^i_{1,K_2} = O(h^6). \tag{58}$$

Thus cancellation happens for a pair of symmetric triangles and the error for a pair of symmetric triangles is of order h^6. To conclude, we use the assumption made on the structured triangulation of D. Since h is proportional to $1/N$, we have

$$\begin{aligned}E_1(P) &= \sum_{K\in T_h} e_{1,K}(P) = \sum_{\substack{\text{matched}\\ \text{triangles}}} e_{1,K}(P) + \sum_{\substack{\text{unmatched}\\ \text{triangles}}} e_{1,K}(P) \\ &= O(N^2)\ O(h^6) + O(N)\ O(h^5) \\ &= O(h^{-2})O(h^6) + O(h^{-1})O(h^5) = O(h^4).\end{aligned} \tag{59}$$

$\diamond$

Lemma 4.6 *Let P be a point not in Σ. Then the error $E_2(P)$ defined in (31) behaves in $O(h^4)$, $E_2(P) = O(h^4)$.*

Proof The error on the element K is

$$e_{2,K}(P) = \int_\sigma \{\Phi_P(m_K(s,t)) - \Phi_P(\widetilde{m}_K(s,t))\}\, (\partial_s \widetilde{m}_K(s,t) \wedge \partial_t \widetilde{m}_K(s,t)) \text{ d}s \text{ d}t. \tag{60}$$

We write a Taylor expansion of Φ_P at $\widetilde{m}_K(s,t)$, use the expansion $\nabla\Phi_P(\widetilde{m}_K(s,t)) = \nabla\Phi_P(\widetilde{m}_K(0,0)) + O(h)$ and the relation (34) to get

$$\begin{aligned}\Phi_P(m_K(s,t)) - \Phi_P(\widetilde{m}_K(s,t)) &= H^1(s,t)\ \partial_1\Phi_P(\widetilde{m}_K(0,0)) \\ +H^2(s,t)\ \partial_2\Phi_P(\widetilde{m}_K(0,0)) &+ H^3(s,t)\ \partial_3\Phi_P(\widetilde{m}_K(0,0)) + O(h^4) = O(h^3). \quad (61)\end{aligned}$$

Then the error on the element K reads

$$\begin{aligned} e_{2,K}(P) &= \int_\sigma \Big\{ H^1(s,t)\ \partial_1\Phi_P(\widetilde{m}_K(0,0)) + H^2(s,t)\ \partial_2\Phi_P(\widetilde{m}_K(0,0)) \\ &\quad +H^3(s,t)\ \partial_3\Phi_P(\widetilde{m}_K(0,0))\Big\}\Big\{\partial_s\widetilde{m}_K(0,0)\wedge\partial_t\widetilde{m}_K(0,0)\Big\}\ \mathrm{d}s\ \mathrm{d}t + O(h^6) \\ &= O(h^5), \end{aligned} \tag{62}$$

since $\partial_s\widetilde{m}_K(s,t)\wedge\partial_t\widetilde{m}_K(s,t) = \partial_s\widetilde{m}_K(0,0)\wedge\partial_t\widetilde{m}_K(0,0) + O(h^3) = O(h^2)$. Again, for a pair of symmetric triangles $\widehat{K}_1$ and $\widehat{K}_2$ and their corresponding K_1 and K_2 in T_h

$$\begin{aligned} H^i(s,t)|_{K_1} &= -H^i(s,t)|_{K_2}, \\ \partial_s\widetilde{m}_{K_1}(0,0)\wedge\partial_t\widetilde{m}_{K_1}(0,0) &= \partial_s\widetilde{m}_{K_2}(0,0)\wedge\partial_t\widetilde{m}_{K_2}(0,0). \end{aligned} \tag{63}$$

With the same argument already used in the last proof to sum over the N^2 triangles of the triangulation, we obtain $E_2(P) = O(h^4)$. $\diamond$

Collecting the results of both Lemmas 4.5 and 4.6, we easily deduce a major result of our paper.

Proposition 4.1 *We assume that the triangulation $\widehat{T}_h$ is structured in the sense precised at the beginning of the section and that $P \notin \Sigma$. Then the error $E(P)$ in (29) behaves in h^4, $E(P) = O(h^4)$.*

Remark 4.1 So far we have fixed the point P and got estimates for the error $E(P)$. We can wonder what happens when P is getting closer and closer to Σ. We know that the integrand Φ_P behaves like $1/d^2$ where d is the distance from P to the boundary Σ. It is advisable then to take into account this behavior in the error analysis.

We assume now that the point P is at a distance $O(h)$ from Σ. Then we can check that the error $E(P)$ in (30) behaves in $O(h^2)$. To prove it we need to slightly modify the previous study. Let d_K denotes the distance from P to a triangle $K \in T_h$ and $d = \min_{K\in T_h} d_K$.

We use the same notations and results as in Section 4.3 to investigate the two error terms E_1 and E_2 in (30). Expanding $\Phi_P(m_K(s,t))$ at $(s,t) = (0,0)$ and using Lemmas 4.1 and 4.2, we obtain

$$e_{1,K} = O(\frac{h^5}{d_K^3}). \tag{64}$$

The next step is to add errors over all K. A special attention is given to the way this summation is done. For triangles *far away* from P ($d_K >> h$) we have a global error in $O(h^4)$. Let us consider the set $\mathcal{T}'_h$ of triangles close to P. Let K_0 be the triangle in T_h such that $d = \mathrm{dist}(P,\Sigma) = \mathrm{dist}(P,K_0)$. We then consider an arrangement of the triangles in $\mathcal{T}'_h$ depending on their distance to K_0. Let V_n, $n = 1,\cdots,\mathcal{N}$ be the set of all the triangles K in $\mathcal{T}'_h$ at a distance r_K from K_0 such that $(n-\frac{1}{2})h \le r_K \le (n+\frac{1}{2})h$. The number of triangles in V_n is an affine function of n for an uniform triangulation. Moreover, we have the following approximation, $d_K^2 \approx r_K^2 + d^2 \approx n^2\ h^2 + c^2\ h^2 = (n^2 + c^2)\ h^2$.

Finally we sum over the triangles in $\mathcal{T}_h'$

$$\sum_{n=1}^{\mathcal{N}} \sum_{\widehat{K}\in V_n} e_{1,K}(P) = \sum_{n=1}^{\mathcal{N}} \sum_{\widehat{K}\in V_n} O(\frac{h^5}{d_K^3}) = \sum_{n=1}^{\mathcal{N}} (a\ n + b) O(\frac{h^5}{d_K^3}) = O(h^2). \tag{65}$$

The estimate for $E_2(P)$ uses the same techniques. $\diamond$

4.4 Error estimate for $\mathcal{B}(P) - \mathcal{B}_h^{\mu}(P)$

In Section 4.3, we considered the computation of (22) by evaluating the integrals exactly. Here we will examine the error when the integrals are evaluated numerically by using the quadrature rule (27). The error $E(P) = \mathcal{B}(P) - \mathcal{B}_h^{\mu}(P)$ is given by

$$\begin{aligned} E(P) \;&=\; \sum_{K\in T_h} \int_\sigma \Phi_P(m_K(s,t))\,(\partial_s m_K(s,t)\wedge \partial_t m_K(s,t))\ \ \mathrm{d}s\ \mathrm{d}t \\ &\quad - \sum_{K\in T_h} \sum_{j=1}^{\mu_d} \omega_j \Phi_P(\widetilde{m}_K(u_j))(\partial_s \widetilde{m}_K(u_j)\wedge \partial_t \widetilde{m}_K(u_j)), \end{aligned} \tag{66}$$

and can be decomposed as $E = E_0 + E_1 + E_2$, where

$$\begin{aligned} E_0 \;&=\; \sum_{K\in T_h} \int_\sigma \Phi_P(m_K(s,t))\,(\partial_s m_K(s,t)\wedge \partial_t m_K(s,t))\ \ \mathrm{d}s\ \mathrm{d}t \\ &\quad - \sum_{K\in T_h} \sum_{j=1}^{\mu_d} \omega_j \Phi_P(m_K(u_j))\,(\partial_s m_K(u_j)\wedge \partial_t m_K(u_j))\,, \\ E_1 \;&=\; \sum_{K\in T_h} \sum_{j=1}^{\mu_d} \omega_j \Phi_P(m_K(u_j))\,\{\partial_s m_K(u_j)\wedge \partial_t m_K(u_j) - \partial_s \widetilde{m}_K(u_j)\wedge \partial_t \widetilde{m}_K(u_j)\}\,, \\ E_2 \;&=\; \sum_{K\in T_h} \sum_{j=1}^{\mu_d} \omega_j\,\{\Phi_P(m_K(u_j)) - \Phi_P(\widetilde{m}_K(u_j))\}\,(\partial_s \widetilde{m}_K(u_j)\wedge \partial_t \widetilde{m}_K(u_j)). \end{aligned}$$

The first term represents the error due to the numerical integration. The other two terms are analogous to E_1 and E_2 in (30) with the integral over σ replaced by the quadrature rule.

Lemma 4.7 *We assume that the triangulation $\widehat{T}_h$ is structured and the numerical integration scheme integrates exactly all polynomials of degree inferior or equal to μ, then E_0 is of order $h^{\tilde{\mu}}$*

$$\textit{where}\quad \tilde{\mu} = \begin{cases} \mu + 2 & \textit{if } \mu \textit{ est even,} \\ \mu + 1 & \textit{if } \mu \textit{ est odd.} \end{cases}$$

Proof Our proof follows the one in [8] and is completely detailed in [4]. Let $G(s,t) = \Phi_P(m_K(s,t))\,(\partial_s m_K(s,t)\wedge \partial_t m_K(s,t))$. Then,

$$E_0 = \sum_{K\in T_h} \left\{ \int_\sigma G(s,t)\ \ \mathrm{d}s\ \mathrm{d}t - \sum_{j=1}^{\mu_d} \omega_j G(s_j,t_j) \right\}. \tag{67}$$

The Taylor expansion of $G(s,t)$ in the neighborhood of the origin gives

$$G(s,t) = H^0_\mu(s,t) + H^1_\mu(s,t) + H^2_\mu(s,t), \tag{68}$$

with

$$\begin{aligned}
H^0_\mu(s,t) &= \sum_{k=0}^{\mu} \left(s\frac{\partial}{\partial s} + t\frac{\partial}{\partial t} \right)^k G(0,0), \\
H^1_\mu(s,t) &= \frac{1}{(\mu+1)!} \left(s\frac{\partial}{\partial s} + t\frac{\partial}{\partial t} \right)^{\mu+1} G(0,0), \\
H^2_\mu(s,t) &= \frac{1}{(\mu+1)!} \int_0^1 (1-\nu)^{\mu+1} \frac{d^{\mu+2}G}{d\nu^{\mu+2}}(\nu s, \nu t)\ \mathrm{d}\nu.
\end{aligned}$$

Since $H^0_\mu(s,t)$ is a polynomial of degree μ it is integrated exactly. Thus, the error can be decomposed as $E_0 = \sum_{K \in T_h} e^1_K + e^2_K$, where

$$\begin{aligned}
e^1_K &= \int_\sigma K^1_\mu(s,t)\ \mathrm{d}s\ \mathrm{d}t - \sum_{j=1}^{\mu_d} \omega_j K^1_\mu(s_j,t_j), && (69)\\
e^2_K &= \int_\sigma K^2_\mu(s,t)\ \mathrm{d}s\ \mathrm{d}t - \sum_{j=1}^{\mu_d} \omega_j K^2_\mu(s_j,t_j). && (70)
\end{aligned}$$

The error term e^2_K can be written as

$$e^2_K = \int_0^1 \frac{(1-\nu)^{\mu+1}}{(\mu+1)!} \left\{ \int_\sigma \frac{d^{\mu+2}G}{d\nu^{\mu+2}}(\nu s, \nu t)\ \mathrm{d}s\ \mathrm{d}t - \sum_{j=1}^{\mu_d} \omega_j \frac{d^{\mu+2}G}{d\nu^{\mu+2}}(\nu s_j, \nu t_j) \right\} \mathrm{d}\nu. \tag{71}$$

By using Liebnitz formula one can show that

$$\frac{d^{\mu+2}G}{d\nu^{\mu+2}}(\nu s, \nu t) = O(h^{\mu+4}). \tag{72}$$

It then follows readily that $e^2_K = O(h^{\mu+4})$.

For the error term e^1_K, a similar argument leads to the estimate $e^1_K = O(h^{\mu+3})$. Summing the two error terms over the N^2 triangles of the triangulation gives a global error of order $h^{\mu+1}$. Then the lemma is proved if μ is odd. If μ is even the estimate can be improved by considering pairs of symmetric triangles. Let $\widehat{K}_1$ and $\widehat{K}_2$ be a pair of symmetric triangles and K_1, K_2 their corresponding triangles in T_h, then one can show that $e^1_{K_1} + e^1_{K_2} = 0$. The estimate is obtained by summing the error term e^1_K over the N^2 triangles collecting the pairs of symmetric triangles as in the proof of Lemma 4.5.

$\diamond$

Lemma 4.8 *We assume that the triangulation $\widehat{T}_h$ is structured and the numerical integration scheme integrates exactly all polynomials of degree inferior or equal to μ with $\mu \geq 2$, then E_1 is of order h^4.*

Proof The error on the element K is

$$e^\mu_{1,K} = \sum_{j=1}^{\mu_d} \omega_j \Phi_P(m_K(u_j)) \left\{ \partial_s m_K(u_j) \wedge \partial_t m_K(u_j) - \partial_s \widetilde{m}_K(u_j) \wedge \partial_t \widetilde{m}_K(u_j) \right\} \tag{73}$$

We use the relations (42) and (55) to expand the two terms $\partial_s m_K(u_j) \wedge \partial_t m_K(u_j) - \partial_s \widetilde{m}_K(u_j) \wedge \partial_t \widetilde{m}_K(u_j)$ and $\Phi_P(m_K(u_j))$. We get

$$\begin{aligned}\Phi_P(m_K(u_j))\,\{\partial_s m_K(u_j) \wedge \partial_t m_K(u_j) - \partial_s \widetilde{m}_K(u_j) \wedge \partial_t \widetilde{m}_K(u_j)\} = \\ \Phi_P(m_K(0,0))\,\{E_4(u_j) + E_5(u_j)\} \qquad (74)\\ + \{s\ \nabla\Phi_P(m_K(0,0)) \cdot \partial_s m_K(0,0) + t\ \nabla\Phi_P(m_K(0,0)) \cdot \partial_t m_K(0,0)\}\, E_4(u_j) + O(h^6).\end{aligned}$$

Since E_4 is a polynomial of degree 2 in the variables (s,t), it is integrated exactly if $\mu \geq 2$. Then from Lemma 4.2 we have

$$\sum_{j=1}^{\mu_d} \omega_j E_4(u_j) = \int_\sigma E_4(s,t)\ \mathrm{d}s\ \mathrm{d}t = 0. \qquad (75)$$

Thus,

$$\begin{aligned} e_{1,K}^{\mu} &= \sum_{j=1}^{\mu_d} \Phi_P(m_K(0,0)) E_5(s,t) + \{s\ \nabla\Phi_P(m_K(0,0)) \cdot \partial_s m_K(0,0) \\ &\quad + t\ \nabla\Phi_P(m_K(0,0)) \cdot \partial_t m_K(0,0)\}\, E_4(s,t) + O(h^6), \qquad (76)\end{aligned}$$

which is the analogous of (56). The result is then derived by considering the pairs of symmetric triangles as in the proof of Lemma 4.5. $\diamond$

Lemma 4.9 *We assume that the triangulation $\widehat{T}_h$ is structured. Then E_2 is of order h^4.*

Proof To get this result one has to follow the proof of Lemma 4.5 with the exact integration replaced by the quadrature rule. This result is not affected by the degree of precision of the numerical scheme. $\diamond$

Collecting the results of Lemmas 4.7, 4.8, and 4.9 we deduce the error estimate for $B(P) - B_h^{\mu}(P)$.

Proposition 4.2 *We assume that the triangulation $\widehat{T}_h$ is structured and that the numerical integration scheme integrates exactly all polynomials of degree inferior or equal to μ with $\mu \geq 2$. Then if $P \notin \Sigma$ the error $E(P)$ in (66) behaves in h^4, $E(P) = O(h^4)$.*

Remark 4.2 One can show that for a point P closed to Σ we still have $E_1(P) = O(h^2)$ and $E_2(P) = O(h^2)$ in (66). However due to the quasi-singular behavior of the integrand, we have $E_0(P) = O(1)$ and the method does not converge anymore. $\diamond$

5 Numerical results

When the domain Ω is a ball, then an analytical expression is known for the magnetic field induced by a uniformly magnetized ball. Then we can illustrate some of the results we have mentioned. The ball has a radius of 1 cm and a magnetization $M = 795$ Ampere per meter ($\chi_m = 10^{-3}$ usi , $B_0 = 1$ Tesla).

5.1 Convergence rate

To illustrate the convergence rate of the method shown in Proposition 4.2, we consider a point P at a distance of 2 radius from the center of the ball. The magnetic field is computed at that point with meshes having an increasing number of triangles. In Figure 3 we present the logarithm of the error versus the logarithm of the number N of triangles. As h is proportional to $1/\sqrt{N}$ we numerically observe a convergence rate of order h^4.

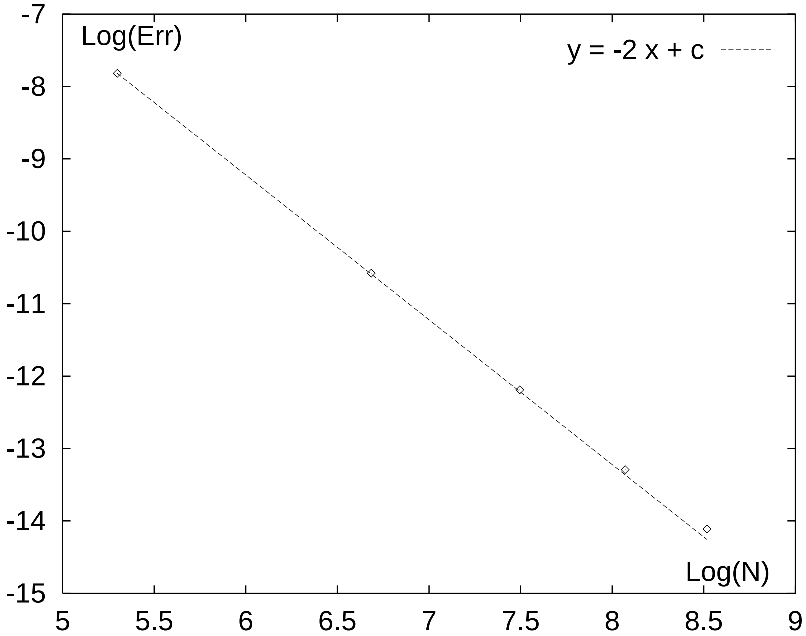

Figure 3: Error as a function of the number of triangles for a point far from the boundary.

5.2 Handling the quasi-singularity

As discussed before, the integrand in (22) is quasi-singular, leading to numerical difficulties when the point P is close to the surface Σ. In Figure 4 we present the relative error versus the distance between Σ and the points P. The different curves correspond to the different integration schemes we are using: the $3 - points$ rule (26) and the $7 - points$ quadrature rule (28) with a varying number l of subdivisions for the parametrization domain σ. The number of triangles used to mesh the surface Σ is 648 giving $h \approx 2.2$ mm. One can observe that up to a distance of $3h$, the $3 - points$ rule is accurate enough. For points closed to the boundary Σ ($d \approx h/2$) the error increases. A way to obtain better results for these points is to refine the mesh of the surface.

5.3 Numerical examples

We present some computational results for 3 test objects: the ball, the cylinder and the cube, illustrating 3 ways of computing the induced magnetic field. For the ball, an approximation of the surface with a piecewise quadratic interpolation is required and the integral over each triangle is computed using numerical quadrature rules. For the cube, the boundary is piecewise flat and we use a mesh of the surface made of 12 flat triangles (they are obtained by dividing each face in 2 triangles). The integral over each triangle is calculated analytically giving a very accurate value for the magnetic field. For the cylinder, the two methods are used altogether. A quadratic interpolation is used to approximate the lateral side of the cylinder and the corresponding integrals are evaluated numerically. The top and the bottom parts can be meshed with flat triangles (except for those on the exterior ring) and the integrals can be calculated analytically. Figure 5 shows the 3 meshes. The sphere (radius 1 cm) is meshed with 680 triangles. The cube (side length 1 cm) is meshed with 12 triangles and the cylinder (radius 1 cm, height 5 cm) with 320 triangles. For the computation we have assumed that these 3 bodies had a magnetic susceptibility

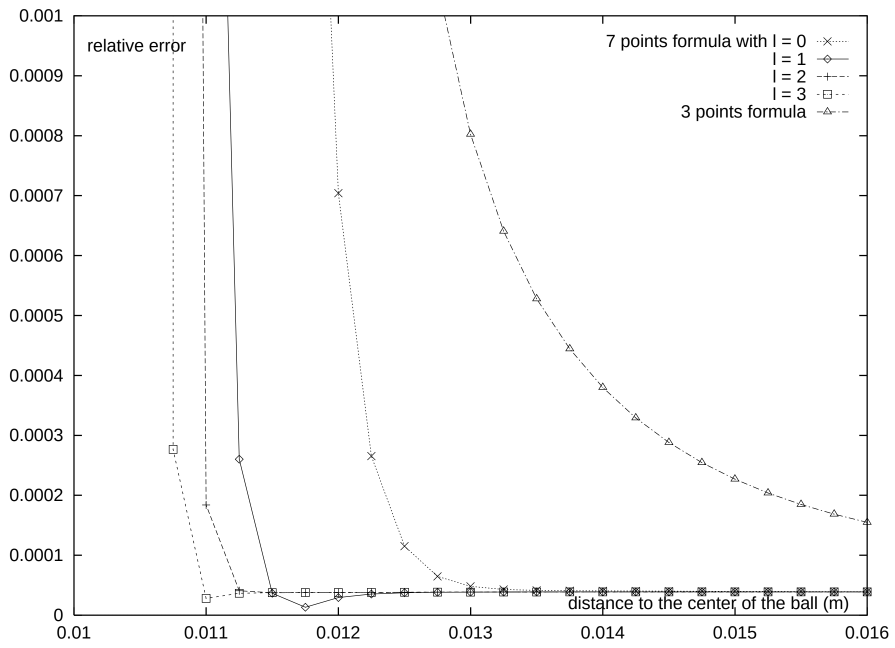

Figure 4: Error as a function of the distance to the center of the sphere. The boundary is located at $d = 0.01$ m.

χ_m of 10^{-3} usi and that they were embedded in an applied magnetic field $\overrightarrow{B_0}$ along the Y axis of 1 Tesla. We have computed the induced magnetic field for 128^2 points in a plane parallel to (O, X, Y) and passing through each body at half its height. Figure 5.3 shows the component of the induced magnetic flux $\overrightarrow{B'}$ along Y. Computations were done on a `Sun Enterprise 450`. Computation requires 184 sec. for the ball, 15 sec. for the cube and 186 sec. for the cylinder.

6 Conclusion

In this paper we have analysed a method to compute the magnetic field induced by a paramagnetic or diamagnetic body embedded in a uniform external magnetic field. The method is based on an integral representation formula for the induced magnetic flux. To compute the integral, we use both numerical quadrature rules and analytical computations. The curved panels of the boundary are approximated with a piecewise quadratic interpolation and numerical quadrature rules are used. The flat panels of the boundary are meshed with triangles of maximal size and the integral over each of these triangles is calculated analytically. This allows both high accuracy and low computation time, requirements that are not fulfilled when using standard numerical methods to solve this problem. These requirements are of great practical importance since the method is used to numerically simulate magnetic susceptibility artifacts in MRI [4], [5].

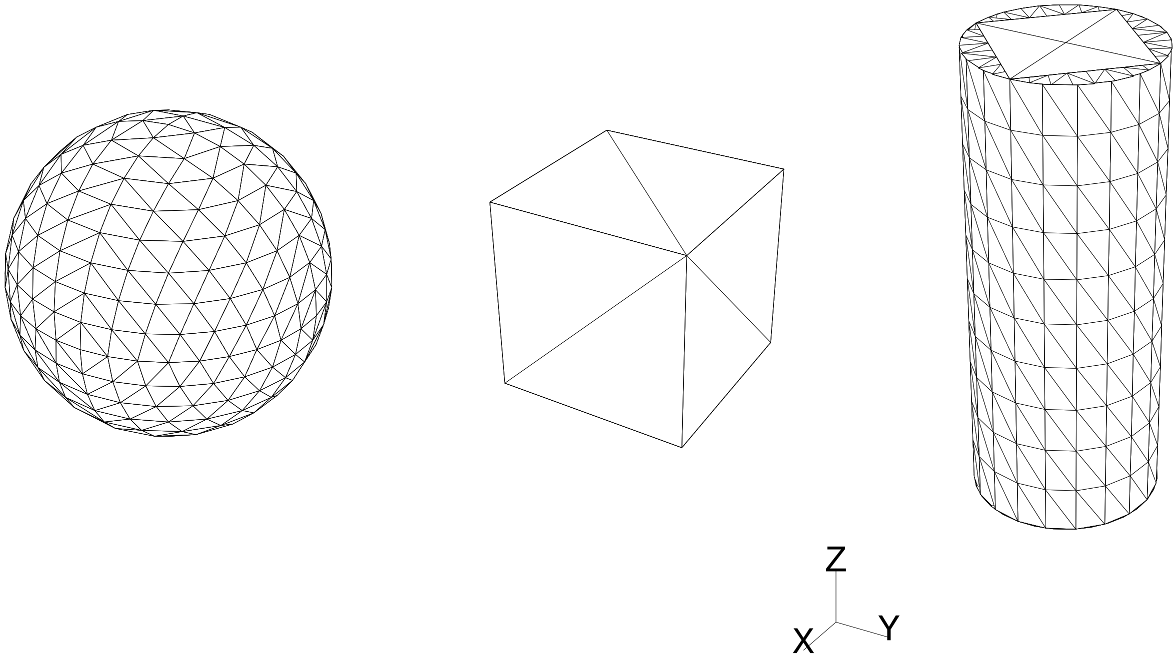

Figure 5: Mesh of the sphere (680 triangles), of the cube (12 triangles) and of the cylinder (320 triangles).

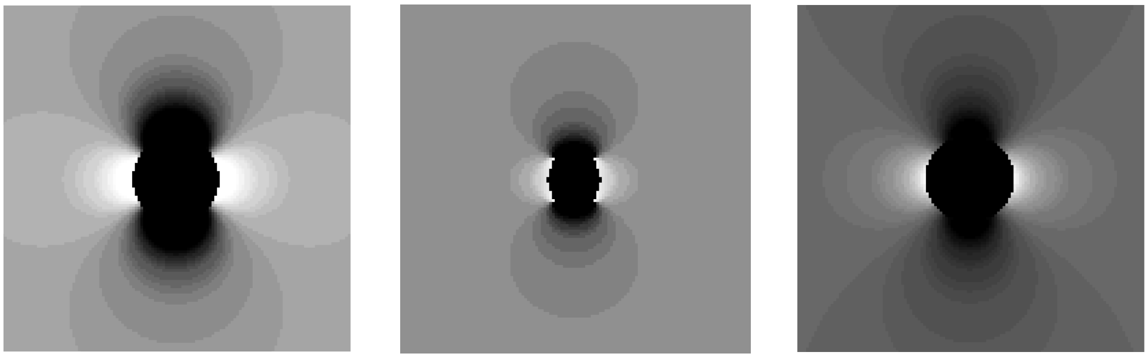

Figure 6: Component of the induced magnetic flux B' along Y in a plane parallel to (O,X,Y) and passing at half the height of each of the 3 geometries (from left to right: the ball, the cube, the cylinder).Each picture corresponds to a square of length 8 cm.

References

[1] K.E. Atkinson. Piecewise polynomial collocation for integral equations on surfaces in three dimensions. *J. Integral Equations*, 9:25–48 (suppl.), 1985.

[2] K.E. Atkinson. User's guide to a boundary element package for solving integral equation on piecewise smooth surface. Reports on computational mathematics 44, Dept of Mathematics, University of Iowa, 1994.

[3] K.E. Atkinson and D. Chien. Piecewise polynomial collocation for boundary integral equations. *SIAM J. Sci. Comput.*, 16:651–681, 1995.

[4] S. Balac. *Artefacts de susceptibilité magnétique en IRM: étude du problème de magnétostatique et simulation numérique.* PhD thesis, Université de Rennes 1, Rennes, France, 1997.

[5] S. Balac and G. Caloz. Magnetic susceptibility artifacts in magnetic resonance imaging: Calculation of the magnetic field disturbances. *IEEE Trans. Magn.*, 32:1645–1648, 1996.

[6] G. Chen and J. Zhou. *Boundary element methods.* Computational Mathematics and Applications. Academic Press, 1992.

[7] D. Chien. *Piecewise polynomial collocation for integral equations on surface in 3-D.* PhD thesis, University of Iowa, Iowa, USA, 1993.

[8] D. Chien. Numerical evaluation of surface integrals in three dimensions. *Math. Comput.*, 64:727–743, 1995.

[9] R. Dautray and J.L. Lions, editors. *Mathematical analysis and numerical methods for science and technology.* Springer-Verlag, Berlin, 1990.

[10] T.H. Duong. A finite element method for the double-layer potential solutions of the Neumann exterior problem. *Math. Methods Appl. Sci.*, 2:191–208, 1980.

[11] M.J. Friedman. Mathematical study of the nonlinear singular integral magnetic field equation I. *SIAM J. Appl. Math.*, 39:14–20, 1980.

[12] B. Heise. Analysis of a fully discrete finite element method for a nonlinear magnetic field problem. *SIAM J. Numer. Anal.*, 31(3):745–759, 1994.

[13] Q. Huang and T. A. Cruse. Some notes on singular integral techniques in boundary element analysis. *Int. J. Numer. Methods Eng.*, 36:2643–2659, 1993.

[14] J.D. Jackson. *Classical electrodynamics.* Wiley, 1975.

[15] P.G. Morris. *Nuclear magnetic resonance imaging in medecine and biology.* Clarendon Press, Oxford, 1986.

[16] J. Pasciak. A new scalar potential formulation of the magnetostatic field problem. *Math. Comput*, 43:433–445, 1984.

[17] Z. Ren, F. Bouillault, A. Razek, and J.C. Vérité. An efficient semi-analytical integration procedure in three dimensional boundary integral method. *COMPEL*, 7:195–205, 1988.

[18] A. Stroud. *Approximate calculation of multiple integrals.* Prentice-Hall, New Jersey, 1971.